Lipidomic Profiling of Algae with Microarray-MALDI-MS towards Ecotoxicological Monitoring of Herbicide Exposure

Peter V. Shanta[1], Bochao Li[1], Daniel D. Stuart[2] and Quan Cheng[1,2,*]

[1]Environmental Toxicology and [2]Department of Chemistry
University of California, Riverside, CA 92521

[*]Corresponding author: Quan Cheng

Tel: (951) 827-2702

Fax: (951) 827-4713

Email: quan.cheng@ucr.edu

Keywords: Lipidomics, MALDI-MS, Herbicide, Algae, Cytotoxicity, Ecotoxicological Analysis

ABSTRACT:

Misuse of agrochemicals has a long-lasting negative impact on aquatic systems. Mismanagement of herbicides in agri-food sectors is often linked to simultaneous decline in the health of downstream waterways. However, monitoring of herbicide levels in these areas is a laborious task, and modern analytical approaches, such as solid phase extraction liquid chromatography mass spectrometry (SPE-LC-MS) and enzyme-linked immunosorbent assay (ELISA), are low throughput and require significant sample preparation. We report here the use of microchip technology in combination with matrix-assisted laser desorption ionization mass spectrometry (MALDI-MS) for assessment of the ecotoxicological effect of agrochemicals on aquatic species at the single cell level. This approach quantifies the fluctuations in lipid content in sentinel organisms and targets a microalga, *Chlamydomonas reinhardtii* (*C. reinhardtii*) as the model system. Specifically, we investigated the cytotoxicity of three herbicides (atrazine, clomazone, and norflurazon) on *C. reinhardtii* by analyzing lipid component variation upon assorted herbicide exposure. Lipidomic profiling reveals significantly altered lipid content at >EC_{50} in atrazine exposed cells. The response for norflurazon showed similar trends, but diminished in magnitude, while the result for clomazone was near muted. At lower herbicide concentrations digalactosyldiacylglycerols (DGDGs) showed a rapid decrease in abundance, while several other lipids displayed a moderate increase. The microchip-based MALDI technique demonstrates the ability to achieve lipidomic profiling of aquatic species exposed to different stressors, proving effective for high-throughput screening and single cell analysis in ecotoxicity studies.

Synopsis:

A platform for whole cell lipidomics analysis using microchip enhanced MALDI mass spectrometry that investigates cytotoxic effects of herbicides on lipid systems with algae *Chlamydomonas reinhardtii*.

INTRODUCTION:

Despite advances in agri-administration practice and industrial safeguards, contamination of waterways and watersheds has resulted in a significant loss of species richness in aquatic systems.[1, 2] For example, misuse of herbicides in agri-food sectors is frequently associated with precipitous decline of health in downstream waterways, closure of public areas, and reputational damage to negligent growers and chemical manufactures.[2, 3] Strategies are needed to monitor the effects of spray drift or runoff of herbicides into non-crop areas adjacent to agricultural zones, and preserve diversity of species in aquatic systems.[4-8] Analysis of chemical risk has traditionally relied on analytical techniques such as SPE-LC-MS and ELISA for quantitative measurement of herbicides, while microcosm studies have been used for the characterization of mortality or inhibition of chlorophyll production in sensitive non-target aquatic species. However, these techniques are low throughput and require a significant amount of sample preparation and long instrument run-times, and little information is provided on the physiological mechanisms that cause chronic or acute toxicity.[7] Surrogate species assays[9] have also been used to monitor bioactivity and bio-inhibition, but they typically require auxiliary measurements, extractions, and chemical standards to understand the biophysical processes responsible for inhibition.

A large number of herbicides are designed to target lipid-based photosystems contained within invasive plant species, which play key roles in terrestrial and aquatic ecology.[2] Lipids are abundant in whole cells, making them an ideal target for cell-based analysis. For chemical and toxicity characterization, lipidomic profiling of sensitive species such as algae that are key members of both terrestrial and aquatic systems has been studied[10]. In conventional approaches, sample is processed by extraction, derivatization, and separation, followed by analysis with multi-capable analytical instrumentations, such as GC-FID, LC-MS, and GC-MS.[5-8, 11-14] The data is then searched against a database (i.e., LipidBlast,[15] Lipid Maps,[16] etc) to identify the subspecies. These techniques, however, are rather laborious, requiring extensive sample preparation, sophisticated separation and/or enrichment procedure, and tedious processing of mass spectral data.

In recent years, MALDI-MS has been used to collect lipid profiles and monitor lipid response to stress,[5, 11, 12, 14] which yields simple mass spectral fingerprints for selective (i.e. targeted) lipid sample analysis. The most common algae lipid classes identified with MALDI-MS are monogalactosyldiacylglycerol (MGDG), digalactosyldiacylglycerol (DGDG), diacylglycerol (DAG), triacylglycerol (TAG), and diacylglyceryltrimethylhomo-Ser (DGTS). Less prominent

lipid classes such as sulfoquinovosyl-diacylglycerol, phosphatidylglycerol, phosphatidylcholine, and phosphatidylethanolamine are also typically identified.[17] Compared to conventional approaches, MALDI-MS has many added benefits: reduced time for sample preparation, less variation from sample handling, and reduced chance of sample degradation, which are common limitations of sample processing. The design of novel substrates and surface functionalities for MALDI-MS has further improved enrichment of cellular targets and enhanced signals.[7, 12, 14, 18, 19]

In chemical and toxicological studies of aquatic environments, specific "omics" processes such as transcriptomics, metabolomics, proteomics, and lipidomics have attracted considerable attention, and work on algae species has shown their sensitivity to environmental toxicants.[5] The extraction of fluorescent photoactive lipids (chlorophylls) and the monitoring of fluorescence has been employed to quantify the effect of herbicides on photosystems in algae.[2] Given that lipids are considered biomarkers for toxicity exposure as alterations in the lipidome can be identified at below cytotoxic levels, these changes are also utilized to trace back biochemical pathways and identify sources of the toxicity effects.[20] An effective approach was developed by Zenobi et al. where micro-array for mass spectrometry (MAMS)[21] was used to investigate metabolomic biomarkers in populations of yeast cells.[22] This technique is attractive as later developments based on similar concepts allow for microbial identification in hospitals settings.[23, 24] Furthermore, it enables straightforward toxicity study where an in-depth understanding of the ecotoxicological impact of herbicides on aqua species can be obtained by monitoring the lipid markers and their response to stimulated exposure. The same group has shown that MAMS is capable of simultaneously enriching, desorbing, and ionizing the most abundant lipids in a single algae cell,[25, 26] and providing phenotypic variations in a limited nitrogen environment.[27] We have recently demonstrated a gold microchip method based on plasmonic enhancement of ionization of low abundance lipid species, allowing for a large lipidome to be identified without extraction.[28] The combination of plasmonic characteristics of gold microarray with MALDI leads to new technical advantages in ionization efficiency and sample localization, making it an ideal platform to study toxicity and cellular response of organisms to photochemical inhibiting molecules at the single cell level.

In this work, we report quantitative monitoring and evaluation of toxicity response in single cell algae to photo-inhibiting herbicides with *Chlamydomonas reinhardtii* (*C. reinhardtii*). *C. reinhardtii* is a well-characterized green alga found in freshwater and damp soils, which is

common in the cultivated fields of North America and Japan, forming a key component of the soil microbiome.[29] Monitoring the toxic effects of chemicals on this ubiquitous, ecologically relevant, and sensitive organism will identify broader implications on the overall health of the ecosystem. Probing the effect of photo-inhibiting herbicides on algae also provides insights into mechanisms by which primary producers are affected and their contribution to ecosystem-wide alterations. The work utilizes a combination of fluorescence and MALDI-MS on a gold micro-chip array for identification of stressed cells by performing lipid profiling. Figure 1 shows the framework for monitoring toxicity in aquatic environments, where *C. reinhardtii* were exposed to varied levels of herbicides. The toxicity of three herbicides (atrazine, clomazone, and norflurazon) was characterized, and statistical analysis was performed to determine indicators of significant toxicity. In addition, we used algae as a surrogate species for lipidomic phenotype cluster analysis (covariant analysis), which led to a cluster-based identification of herbicides. The applicability of the platform for assessing a xenobiotic's general risk to other species with similar ecotoxicological responses is discussed.

EXPERIMENTAL:

Materials:

Super dihydrobenzoic acid, biotechnology certified dimethyl sulfoxide (DMSO), and analytical grade solvents were purchased from Sigma Aldrich. POPC (1-palmitoyl-2-oleoyl-glycero-3-phosphocholine) was purchased from Avanti Polar Lipids, Inc (Alabaster, AL). Atrazine, clomazone, and norflurazon were purchased from AccuStandard Inc. (New Haven, CT). BK7 glass microscope slides came from Fisher Scientific. High purity water (>18 MΩ cm-1) was obtained from a Barnstead E-Pure water purification system. *C. reinhardtii* (+) bacteria-free (#152040), and sterile Algae-Gro® medium were purchased from Carolina Inc (Burlington, NC).

Algae Culture Conditions and 96-Hour Acute Herbicide Toxicity:

Freshwater wild-type algae strain, *C. reinhardtii*, was maintained in a medium at 25˚C with a "cool white" fluorescent illumination on a 12-hour cycle. For analysis of toxicity, the stationary culture was seeded and cultured until exponential to stationary phase (~1-2 weeks). The analysis of growth was spectrophotometrically determined from logarithmic growth at 600 nm. The relationship

between the cell count and absorbance intensity is shown in Figure S1. At the exponential-to-stationary growth phase, the cells were spiked with static concentrations of 3 herbicides, atrazine (5, 10, 50, 100 μM), clomazone (25, 75, 100 μM), or norflurazon (5, 10, 50, 100 μM). Cells were collected at 96-hours post herbicide exposure and washed 3 times using ultrapure water after 5 minutes of centrifugation at 2500 g. Cells were promptly spotted via micro syringe onto gold microchips using an x-y stage on a nanoliter electrodeposition system (Nanoliter Cool Wave Liquid Systems). To quench cell metabolism, the microchips with drying cells were immediately placed into a vacuum desiccator.

Fabrication of the Gold Microchips:

The gold microchip array was fabricated in the Cleanroom Facility at UCR following our previously published procedure.[30] The physical parameters of finished gold μchips are as follows: each well on a gold microchip has a diameter of 800 μm, with the well bottom covered with 50 nm thick gold and the edges of wells covered with 200 nm gold. In brief, glass slides (1 x 3 inches) were cleaned with Piranha solution (H_2SO_4:H_2O_2, 3:1, **Caution!**), rinsed with ultrapure water and ethanol, and dried under nitrogen. The photoresist was then spun-coated onto glass slides and baked at 110 °C. A mask aligner and UV-light were used to pattern the photoresist, followed by development for 45 seconds in a developing solution. Next, e-beam deposition was used to deposit 2/200 nm of Cr/Au onto the arrays. A spray gun filled with acetone was used to remove the photoresist to reveal the array pattern, followed by e-beam deposition of 2/50 nm of Cr/Au onto the surface to produce a pristine gold well array. Freshly made microchips were placed in a vacuum desiccator for storage.

Overview of Workflow: Metal Enhanced Fluorescence and MALDI-MS Lipidomic Analysis

A conventional 96-hour EC_{50} bioassay of ecotoxicity was coupled with gold microarrays for metabolic analysis of toxicity in *C. reinhardtii*. The flow-chart of the method is shown in Figure 1. All tests were conducted after a 96-hour exposure to targeted chemicals. The procedures for gold microchip profiling of algal lipid mass fingerprints were recently published[28]. The method can be broken into four parts: i) sample preparation ii) metal enhanced fluorescence (MEF) facilitated localization, iii) acquisition of lipidomic data by MALDI-MS (MS/MS), and iv) data processing. The gold microarray is an integral part of the substrate design and demonstrated three

major merits: (i) enhanced fluorescence signal[31-33] due to the coupling of surface plasmon with the fluorophore's emission, (ii) enhanced MS/MS due to rapid thermalization of excited electrons (i.e. hot-electron transfer)[34] and generation of laser-induced plasma at near gold ablation thresholds[35] and (iii) robustness of the surface to oxidation, sample processing, and sample archiving.

Fluorescence images and bright-field images of cells were obtained using an epifluorescence microscope equipped with a TRITC filter cube for fluorescence detection of chlorophyll and a QImaging Retiga 1300. FIJI software package (ImageJ) was used to assemble individual fluorescence images into their respective locations on the array. This grid of fluorescence images (320/chip) was interfaced with a template-design using MALDI-MS software (Series Explorer Software). The interface facilitated unambiguous localization of cells within wells, which is necessary for laser targeting with MALDI-MS. This step also eliminated unwanted data acquisitions from wells that did not contain lysed cells for analysis. The microchip was placed on a holder that was modified to accommodate standard 1″x3″ glass slides and loaded into the mass spectrometer. A reflectron AB-Sciex 5800 MALDI-TOF instrument operating in positive mode with a laser fluence of 4500 a.u. was used to collect lipid mass profiles. One spectrum contains m/z values versus intensity (a.u.) that were averaged from 200 shots collected in a continuous linear or v-shaped laser-pattern over a single cell or packet of few cells. The tandem MS spectra were obtained from a scan of global lipid profiles and precursor ion selection of peaks with high resolution and s/n values. A tentative lipid library was compiled from experimental m/z peaks values, MS/MS data, and references. All mean values were calculated from >37 spectra/samples to generate charts, heatmaps, and statistical analysis of the results.

Data Processing and Statistical Analysis

Metaboanalyst software package[36] was utilized to perform the statistical analysis of controls (n > 40) versus herbicide exposures (n > 25), and Prism7 was used to generate volcano plots. Additional information of processing and data analysis is described below in Results and Discussion.

RESULTS AND DISCUSSION:

Assessment of Herbicide Morbidity in an Aquatic System

The herbicides tested here target the photosystems of algae in different ways, with Atrazine targeting photosystem II while clomazone and norflurazon on synthesis of pigments (carotenoids

and chlorophyll). Spectrophotometric based bioassays provide a binary analysis on lethality, which has been extrapolated to determine risk in other organisms that harbor the photosynthetic system in practice[37]. However, they are less effective to trace the cause of changes and cannot directly link the observed change to a particular mode of action that may also affect other organisms in the system. We set to correlate the changes in the lipid profile to the toxicity of the herbicide and identify the herbicide's downstream lipid targets with statistical tools, which is important for pollutant studies in environmental toxicity assessment.

It is reported that atrazine and clomazone concentrations greater than 0.4 nM are common in U.S. streams and groundwater, and a total molecular concentration of atrazine at greater than 10 μM is often observed in consecutive months.[38] The atrazine and norflurazon concentrations in agricultural streams and shallow groundwater can shift even more dramatically based on time of year and region.[38, 39] Spatiotemporal monitoring of downstream rivers associated with tributary agricultural streams revealed atrazine levels frequently exceed the 12.5 μg/mL (58 μM) benchmark set by the US Environmental Protection Agency.[38] While monitoring of surficial-aquifer wells has identified median norflurazon concentrations of 25.0 μg/L and 22.0 μg/L for its degradate dimethyl norflurazon, with the highest concentration reported at 105 μg/L, far exceeding Florida's health-guidance benchmark.[40]

We first characterized the herbicide morbidity for algae *C. reinhardtii* with the three compounds. As shown in Figure 2C, EC_{50} values, ascertained from the dose-response curves of 96-hours post exposure, are 1.2 μM for atrazine, 6.6 μM for norflurazon, and >150 μM for clomazone, respectively. These empirically derived EC values agree relatively well with those in recently published literature[41, 42] for atrazine and norflurazon, while the proherbicide clomazone requires bioactivation to inhibit the isoprenoid pathway, a potentially null bioactivation pathway in *Chlamydomonas*.[43] These differences were further investigated by the lipid profiling experiment that offers a new angle to understand the mechanisms.

Gold Microchip with MEF for MALDI-MS Analysis of Algae Lipidome

Utilizing the plasmonic micro arrays, we conducted surface enhanced MS analysis of *C. reinhardtii* by first locating the cells using MEF, followed by MALDI-MS and MALDI-MS/MS to acquire detailed mass spectra for identifying lipids. For whole cell lipid profiling, the laser beam must be precisely directed to the microorganisms confined to a specific region to enhance the

effectiveness. An alternative method would be MALDI imaging, which turns out to be less ideal for this study as scanning the surface with single- or few-cells would prove daunting in both data analysis and time required for scanning.[44] Furthermore, the resolution of a stand-alone MALDI-MS imaging system has yet to reach a resolution needed for single cell analysis,[17, 45] and the location of cells can only be determined after the scan from MS data. Only a few pixels within the region of a single cell are produced, but recent advances show promise in improving spatial resolution[46]. A straightforward approach that allows convenient localization of the cells prior to MS data collection would be highly useful.

The gold microarray substrate proves to be an ideal surface for that purpose due to marked fluorescence enhancement. It has been reported that a thin gold film of 50 nm in thickness can generate a strong evanescent wave under proper optical configuration.[47, 48] The coupling between the wave and nearby fluorophores located within 20-200 nm from the surface causes a fluorescence enhancing effect. This phenomenon, known as MEF,[49] is broadly observed and used for signal enhancement in fluorescence-based sensing[50]. Algae shows an autofluorescence property due to the presence of chlorophyll a in the membrane, but the signal is usually very weak. MEF substantially improves the fluorescence images (supporting information), makes it simple and clear to pinpoint cells inside the substrate wells. The images were stitched together into a series of images for synchronization with a homebuilt template within the MALDI-MS software, which enabled single cell or multiple cells to be quickly localized for laser ionization in MALDI.

Lipid Profiling and Population Averaging of *C. reinhardtii*

The dysregulation of lipids in microalgae are associated with stress induced genomic regulation[5] or oxidative damage[51] caused by changes in the environment, including nutrient level perturbations, or the presence of harmful exogenous molecules.[52] Lipidome characterization of an indicator species has been used to investigate the impact of exogenous herbicide on microalgae. The most widely used techniques for detailed analysis of the sample's total lipidome involve lipid extraction, chromatographic separation, and ESI-MS ionization.[6-8] Another method is the shotgun approach that combines lipid extraction with direct-infusion ESI.[11, 12] Single cell MALDI-MS method has multiple advantages over the ESI-MS approaches, with straightforward sample preparation being the most attractive one. Our MALDI-MS results show that data from multiple-cell spectra had smaller variation in signal intensity than the single-cell spectra. Nevertheless,

normal population heterogeneity in *C. reinhardtii* is < 5%,[21, 45]. As such we present averaged data obtained from multiple samples that are representative of the entire population (n > 25), which fits the purpose of the current study that is focused on characterization, identification, and quantitation of toxicity in an algae population. Heterogeneity is incorporated into the statistical variance that is accounted for in later studies. Our results also revealed that the level of variation within a typical population is minimal compared to the *C. reinhardtii*'s response to herbicide. All spectra were obtained from cells that were taken from biological replicates and non-herbicide containing controls. From this point forward, single cell data spectra (n > 25) were analyzed for clustering linkages and significance of lipid class change.

Table 1 summarizes the lipid species of *C. reinhardtii* identified by microarray MALDI-MS. The parenthesis represents R_1 and R_2 groups acyl chain residues of varying lengths. The assignments of the lipids are in agreement with those made by others,[25, 53-57], including those using lipophilic extraction to characterize *C. reinhardtii*'s lipid profiles.[53-58] From the results, the ionization of chlorophylls $[M\text{-}Mg^{+}+3H]^{+}$ is clearly suppressed. Chlorophylls is commonly a major peak that obscures low abundance lipid species, whereas its suppression allows identification of many other low abundance lipids. In addition, a substantial increase in ionization efficiency of other lipids is observed, likely through a combination of ion suppression, sample confinement, and metal enhancement effects.[28] This facilitated the assignment of many peaks not previously detectable under similar conditions in a single mass spectrum. While the general consensus has been that efficient ionizers such as chlorophyll[59] should be separated *ex-situ* from samples before ionization experiments, this process is no longer necessary using the gold microarrays.

Data Explorer software was used to mass calibrate the spectrum and export text files. An open source software known as *mMass*[60] was used to obtain m/z, baseline, peak values (S/N > 5), and conduct a preliminary lipid search to identify lipids from the Lipidmaps®[16] library. Precursor ions were selected from the profile and CID-MS was used to confirm lipid classes. For CID-MS analysis, the precursor ion window was set to ± 0.2-1.5 m/z units, with the window size being contingent on the presence and abundance of nearby peaks. We found that DGDGs, MGDGs, DGTS, and TAGs were efficiently desorbed from the gold surface, while DAGs were ionized to a lesser extent (Figure 3). Previous work has found MALDI-MS is a useful technique to identify and compare TAG and DGDG levels from 500 mL culture of cells using separation, which is not possible with GC-MS due to low abundance and instability of derivatized compounds.[57]

For spectra analysis, weak signals at 871.57 m/z and 885.55 m/z are assigned to light capturing molecules chlorophyll a $[M\text{-}Mg^{+}+3H]^{+}$ and chlorophyll b $[M\text{-}Mg^{+}+3H]^{+}$, respectively. The most abundant DGDG and TAG species are assigned to Na^{+} and K^{+} adducts of DGDG (34:3), TAG 54:3, and TAG 54:2. MS/MS fragmentation was conducted for analysis of the most abundant lipid subspecies, from DGDG, TAG, DGTS, and MGDG. The microchips are highly selective to the ionization of DGDG and TAG compounds, because polar and neutral compounds easily adduct with cationic sodium to form stabile positive ions. Both Na^{+} and K^{+} adducts of DGDG and TAG were identified in the lipid mass profile, and fragmentation of precursor ions confirmed identification and elemental analysis of acyl side chains. DGTS lipids were identified as only protonated adducts; this may likely be due to DGTS's zwitterionic nature and the acidic matrix environment.

Figure 4 shows a quantitative analysis to evaluate lipid concentrations and determine percent concentration of lipid subspecies. In this work, the relative percent concentration measurements ($n > 25$ and peaks = 60) of each lipid were performed. The data obtained by the MEF/MALDI-MS μchip method has been compared to previously published research using LC-ESI-MS and they agree well with this work. In Figure 4A and 4B abundance of various DGDG lipid species can be seen compared across increasing herbicide concentrations, indicating species that are most affected by associated herbicide treatment. There is limited change in lipid abundance across lipid species for clomazone affected algae except at the highest concentration of 150 μM where a decrease in DGDG (36:3), DGDG (36:4), and DGDG (36:5) is seen. While for norflurazon abundant lipid species DGDG (34:3) and DGDG (34:6) have considerable decreases in lipid abundance upon even low (10 μM) treatment. Also, significant changes in low abundance lipid species such as DGDG (36:2) through DGDG (36:7) can be identified. Significant changes in DGDG lipid species are also seen in atrazine affected algae as shown in previous publication.[28] Volcano plot in (Figure 4D) displays lipid species with significant changes ($P<=0.05$) of two-fold or greater indicated in green for those of decreasing abundance and red for those increasing in abundance.

Evaluation of the Impact of Herbicides on Algae Lipidome: Statistical Analysis

As summarized in Table 1, norflurazon at below benchmark concentrations and near EC_{50} values (1 μM and 10 μM) produced a striking decrease in the overall abundance of all

DGDG compounds in algae after 96 hours (Figure 4). Atrazine demonstrates the same decrease in DGDG compounds[28] while also displaying increases in DGTS and TAG lipid species at and below EC_{50} values followed by a significant decrease for concentrations above the EC_{50} value (Figure S3). Galactolipids (MGDG and DGDG) are major components of photosynthetic membranes that are responsible for cell signaling and membrane structure.[56] In higher plants, di-galactolipids are non-bilayer forming lipids that support protein aggregation in Photosystem II.[61] A similar function of DGDG in green-algae plastids[62] explains the apparent decreasing signal of DGDG lipids in response to norflurazon's inhibition of phytoene desaturase and the subsequent breakdown of the lipid supported photosystem complex (Figure 4). The observed decrease in DGDG was accompanied by an increase in MGDG intensity, which suggests that norflurazon induced stress resulted in a breakdown of DGDG, into lyso-DGDG forms (i.e. MGDG). TAG signals showed an overall increase in number of TAG molecules, by either *de novo* or scavenging synthesis of TAGs, which was a compensatory effect of DGDG signal decreases in *C. reinhardtii* (Table 1). TAG accumulation during stress conditions is a common phenotypic response in many types of algae, which has been reviewed extensively in the literature.[63]

DGTS are nitrogen containing and extraplastidic lipid molecules that have been characterized as a substitute for phosphatidylcholines, and function as a proxy for structural integrity in membranes. Furthermore, studies focused on nitrogen deprivation[54] and heat stress[55] for biofuel production have suggested a varied response, and either a causal decrease[55, 64] or increase[27, 54] effect on the concentration of DGTS lipids. This discrepancy is attributed primarily to temporal analysis of stress, i.e. the length of the experiment[27, 54] (hours to weeks). This is further nuanced by effects from differential lipid remodeling[54], algae in various growth stages[54] and genetic diversity[27]. Our results show that atrazine, a nitrogen-abundant environmental pollutant, resulted in a dramatic increase in the abundance of short-chain DGTS lipids. The increase in DGTS signals agrees with the temporal model in that our examinations were conducted with cultures in the late-stationary growth phase and herbicide stress increased abundance of DGTS. It appears there is a threshold concentration of atrazine, wherein 50 μM and greater, induced a spectrum-wide decrease in lipid signal, and with a post-96-hour exposure, it ultimately leads to a 100% mortality.

For norflurazon treated algae similar changes were identified for DGDG, TAG, and DGTS lipid species. These changes likely follow similar mechanisms to those for atrazine affected algae,

as both herbicides are photosystem II inhibitors. The end result is the same for both herbicides, but the mode of action is different. Norflurazon's effect is propagated through the reduction of carotenoid biosynthesis via inhibition of phytoene desaturase.[65] This distinction can be clearly seen in the difference in EC_{50} values and the extent to which lipid species are up or down regulated. As the EC_{50} for norflurazon is higher this indicates that the bleaching effects caused by norflurazon's phytoene desaturase inhibition either take longer to affect algae lipid systems or are not as directly related to lipid pathways as the electron transport processes affected by atrazine. This is further supported by the regulation of lipid species coinciding with that for atrazine treated algae but to lower extents, thus indicating that the same lipid accumulation and breakdown pathways were activated but with less severity.

Clomazone also targets pigment synthesis but it did not have a significant effect on lipidomic clustering. It has been speculated to require plant-bioactivation to become an active inhibitor in photosynthetic organisms,[66] and thus is possibly a null pathway in *C. reinhardtii*.[66] From the data presented here we can see that clomazone does not get activated within algae and therefore had little effect on algae lipid systems. This is especially clear when compared with norflurazon which significantly altered lipid profiles and targets the same synthesis pathways as clomazone.

To illustrate how each of the lipid variables were affected by herbicides, volcano plots are provided for visualization of the most significant changes in large data sets.[13, 14] As shown in Figure 4, the effect of 10 μM norflurazon ($\log_2$(FC(norflurazon /control)) is characterized by a significant excess of TAG molecules and a decrease in DGDG molecules. A significant change threshold of $P = 0.05$ and $FC > 2$ was used to compartmentalize lipids into the upper left and right corners of the volcano plot. This strategy proved to be highly effective for cell based lipidomic toxicity screening.

We have demonstrated that this microarray technique can characterize differences in lipidomic responses to two different herbicides with similar modes of action. Norflurazon and clomazone are both inhibitors of pigment synthesis, yet their effects on *C. reinhardtii* are strikingly different. Clomazone at very high concentrations had little effect on inhibition of cell growth (Figure 2), and the volcano plot in Figure 4C showed a relatively high concentration (75μM) of clomazone also had little effect on lipid abundance. In comparison, norflurazon saw a significant amount of TAG accumulation and effects on cell growth at a much lower concentration (10 μM).

Hierarchical clustering in Figure 6B shows strong linkage of lipidome composition and physiological response of individual cells exposed to different types of herbicides. Some overlap exists between toxicological response of lipidome to atrazine and norflurazon, which is likely due to the similarities in the two herbicide's modes-of-action (target photosystem II). Unsupervised multivariate principal component analysis (PCA) was used to explain the variance in the data set and distinguish single cell lipid profiles under different herbicide induced stress conditions. There was no separation between clomazone and its control as all of the control values fell within the 95% confidence region of the clomazone data set, which is understandable based on the lack of bioactivation within algae systems. PCA score plots of atrazine and norflurazon versus control showed good separation, and partial least squares discriminate analysis (PLS-DA) was performed to further separate the herbicide groups into distinguishable phenotypic clusters (Figure 6). PLS-DA addresses questions on how well the lipid response profile of *C. reinhardtii* predicts which herbicide is responsible for toxicity. Differentiation of lipid clusters can, therefore, be used to facilitate herbicide classification and may be useful in the prediction or identification of herbicide contamination in polluted waterways and watersheds. Hence, statistical analysis of exposure data obtained from sensitive indicator species can be combined with higher trophic organisms to determine and/or measure environmental health.

In this work, we have reported a new method that combines microarray analysis, sample archiving, fluorescence microscopy, and single cell mass spectrometry to study toxicity of three herbicides. MEF and enhanced MALDI-MS/MS were combined to analyze lipids from whole cells in a high-throughput array format. The results showed that the gold substrate enhances MALDI-MS performance, generating a lipid library that consists of 54 identified lipid species without a purification process. The results indicate these three herbicides have a pronounced and different effect on mass peaks from ecological relevant indicator species, *C. reinhardtii*. Analysis of algal lipid response to atrazine and norflurazon showed a significant reduction in DGDG content at low concentrations. In contrast, subspecies of TAG saw a significant increase of these energy storing lipids. Clomazone with a relatively high EC_{50} had little effect on DGDG levels at the highest concentration tested and showed only a slight increase in TAG levels. The results indicate that lipid conversion during herbicide induced stress conditions in algae leads to TAG accumulation and DGDG depletion. Volcano plots, a viable analysis tool for identifying lipids markedly affected by different herbicides, yields multiple lipid species with statistically significant greater than two-

fold changes. PCA combined with PLS-DA analysis showed that this lipidomic approach can be used to analyze trends in lipid abundance for classification of specific herbicides. The up and down regulation of lipids can be linked to unique herbicide effects and these patterns can then potentially be useful for identifying which herbicides are affecting the algae. Compared to other techniques in the analysis of lipids from cells, this approach is fast as there is no need for extraction. In addition, this approach can be used to study lipid mass profiles in similar cell types and may similarly be extended to variation analysis in those samples, particularly in efforts to monitor the environment. This work demonstrates the effectiveness of plasmonic substrates to enable robust tracking of lipid abundance and signatures upon cellular treatment. Further presenting opportunities to study more complex microorganisms and their reaction to environmental changes.

ACKNOWLEDGMENT

We would like to acknowledge the financial support from NSF (CHE-1413449).

SUPPORTING INFORMATION

Calibration curve for algae cells (Figure S1), fabrication of microarrays (Figure S2), and effect of atrazine on DGTS and TAG lipids (Figure S3). This material is available free of charge via the Internet at http://pubs.acs.org.

Identified Lipid Classes	Lipid Molecular Species Identified	Lipid Class Physiology	EC_{50} At	EC_{50} Nf	EC_{50} Cl
DGDG 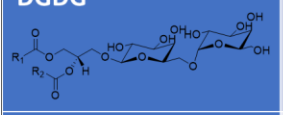	(36:2), (36:3), (36:4), (36:5), (36:7), (34:0), (34:1), (34:2), (34:3), (34:4), (34:5), (34:6), (34:7)	Major components of photosynthetic membranes that are responsible for cell signaling and membrane structure.	↓	↓	nc
TAG 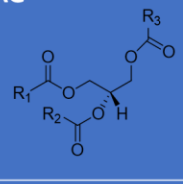	(54:2), (54:3), (54:4), (54:5), (54:8), (52:2), (52:3), (54:4), (54:5), (52:6), (54:7), (54:8), (52:9), (50:1), (50:2), (50:3), (50:4), (50:5), (50:6), (50:7), (48:3)	TAG accumulation during stress conditions is a common phenotypic response	↑	↑	nc
DGTS 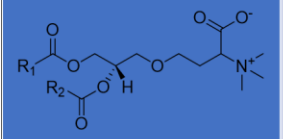	(36:0), (36:1), (36:2), (36:3), (36:4), (34:2), (34:3), (34:4), (32:0), (32:1)	DGTS are nitrogen containing and extraplastidic lipid molecules that have been characterized as a substitute for phosphatidylcholines, and function as a proxy for structural integrity in membranes.	↑	↑	nc

Table 1. A list of lipid classes and species types detected by MALDI-MS. Parenthesis denotes the presence of all isomers with the same number of carbons and double bonds, for example (36:2). Up and down arrows indicate an overall change in lipid abundance at EC_{50} for three herbicides and the resulting impact on cell physiology. At = atrazine, Nf = norflurazon, Cl = clomazone, nc = no change.

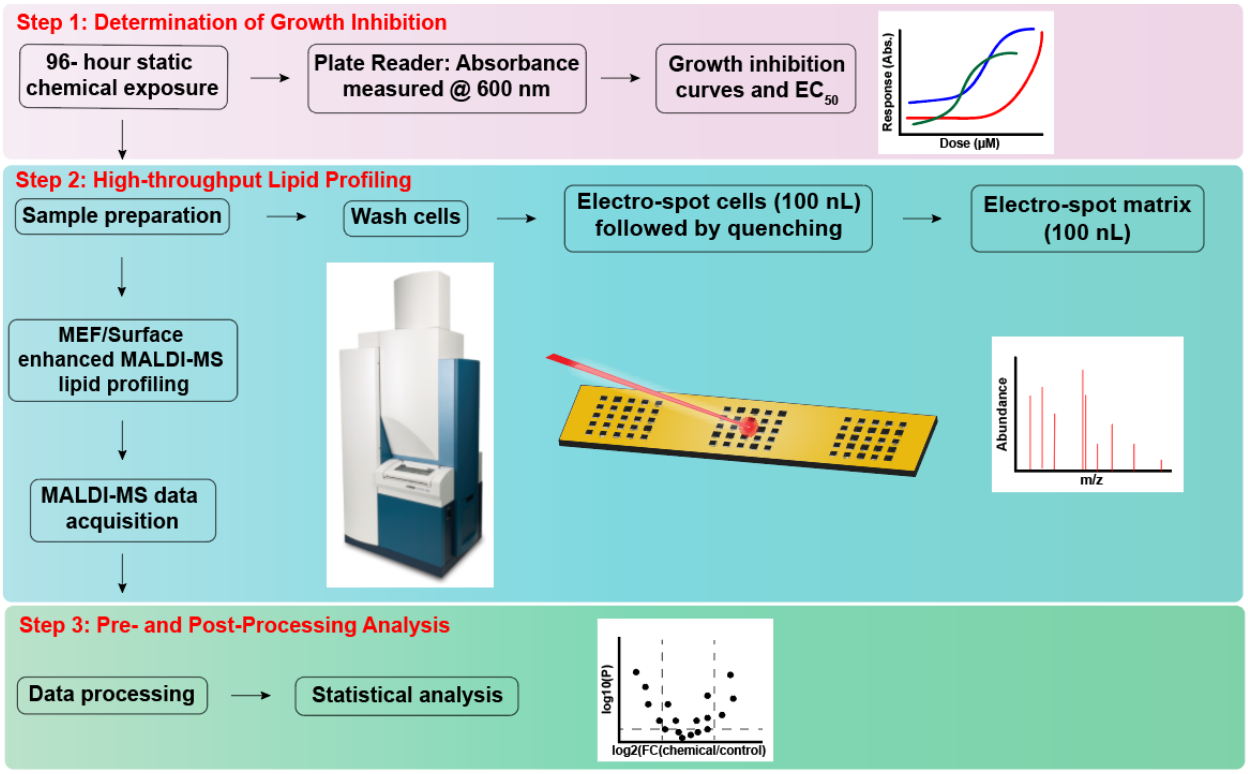

Figure 1. Overview of framework to determine the ecotoxicological ramifications of aberrant herbicides on the lipidome in the indicator species *C. reinhardtii*.

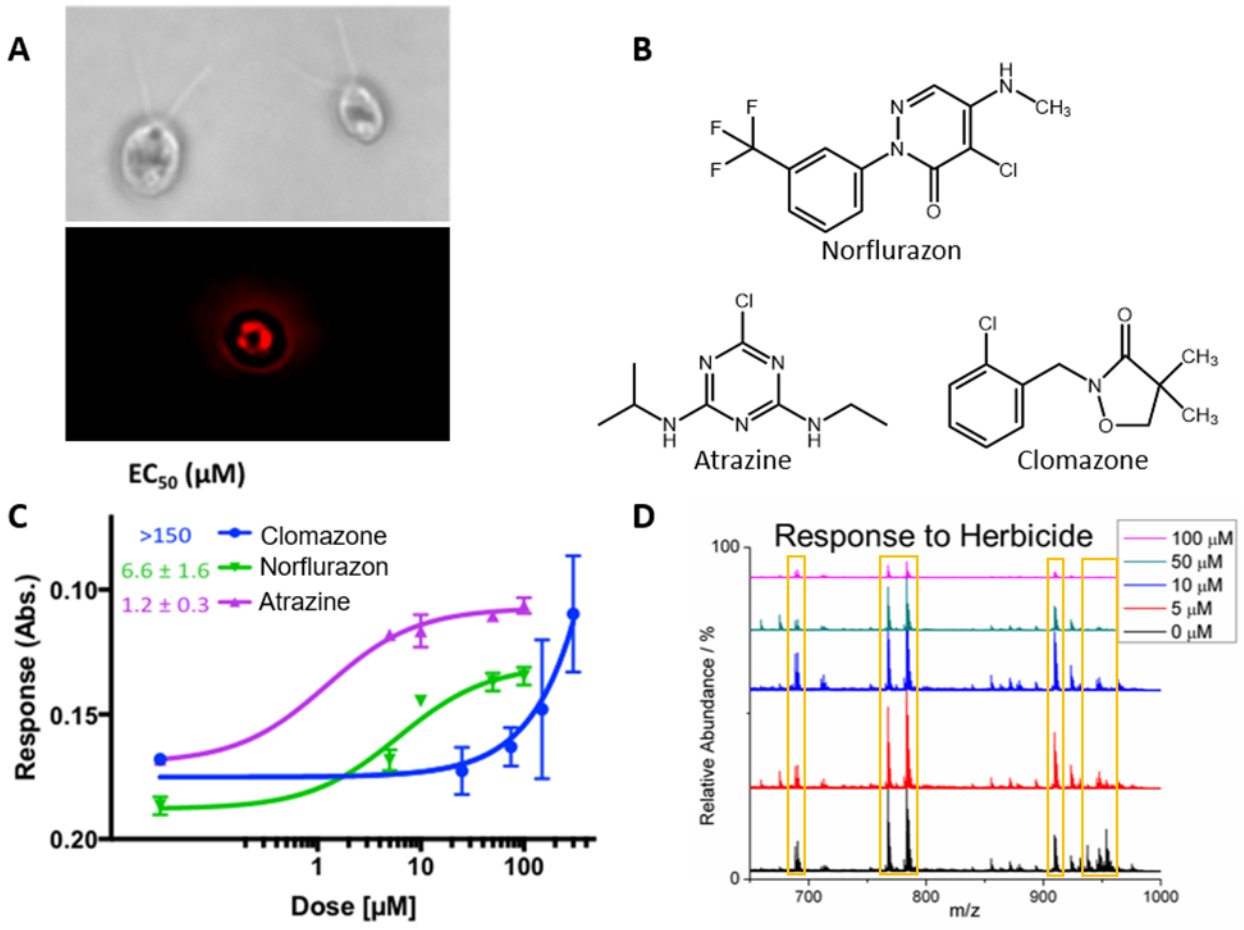

Figure 2. Bright field (top) and fluorescent (bottom) images of C. reinhardtii algae (A). Structure of three herbicides used for exposure tests on algae (B). Herbicide dose-responsive curves for conventional analysis of toxicity and calculation of EC_{50} values. Dose response curves show the algae response upon exposure to different herbicides. EC_{50} of atrazine was measured at 1.2 ± 0.3 µM, norflurazon EC_{50} at 6.6 ± 1.6 µM, and clomazone EC_{50} at >150 µM. (C). Relative abundance of algal lipids associated with atrazine herbicide treatment (D). Ion abundance data from mass spectra are extracted for statistical analysis and to investigate the effects of herbicide on algal lipidome.

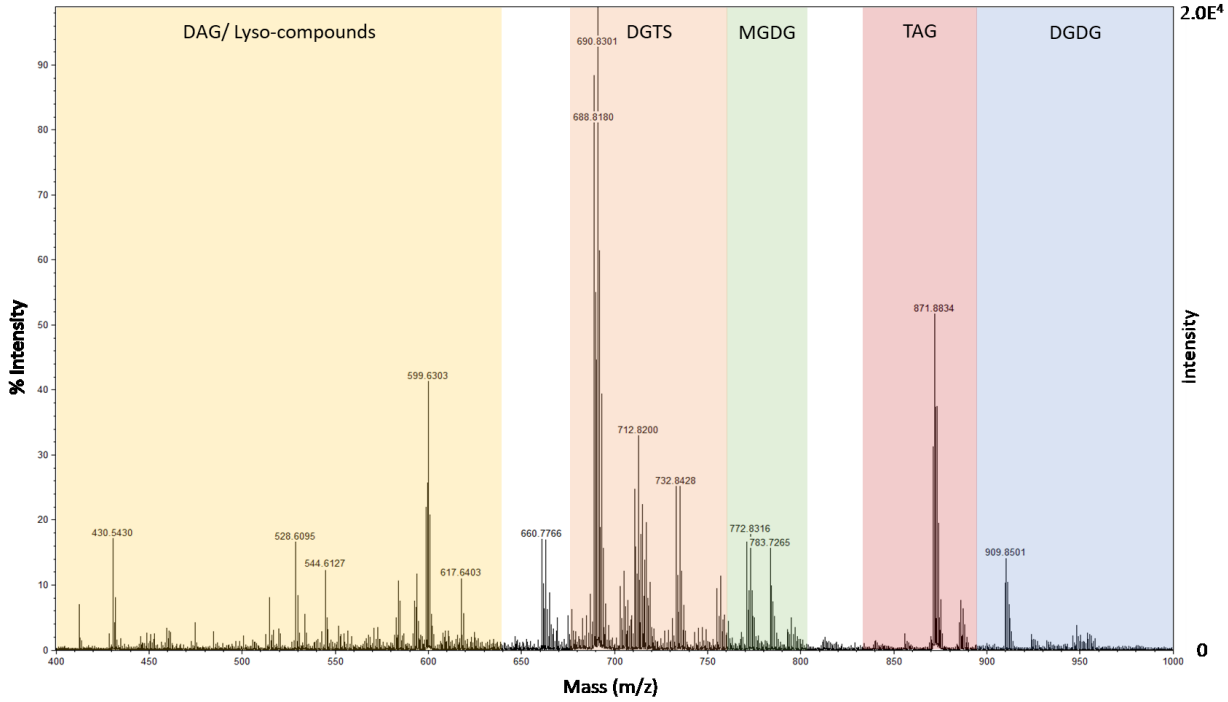

469

470

471 Figure 3. MALDI-MS with distinct m/z regions where the different lipid types are found to form

472 the lipid fingerprint of *C. reinhardtii*.

473

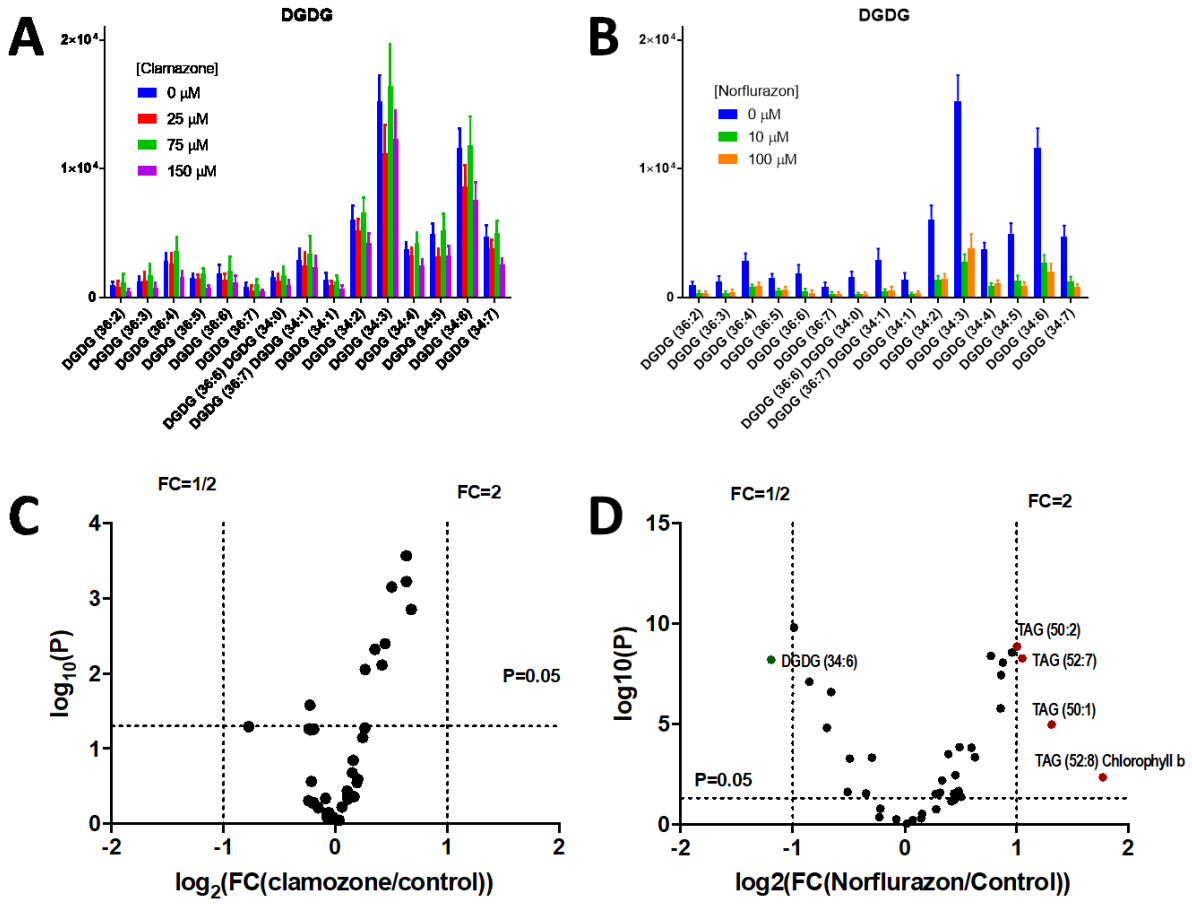

Figure 4. The effect of Norflurazon (A) and Clomazone (B) concentration on digalactosyldiacylglycerol (DGDG) abundance in algae. Statistical analysis of variation in the data reveals significant changes in concentration of lipids after 96 hours in (C) 75 µm of clomazone and (D) 10 µm of norflurazon.

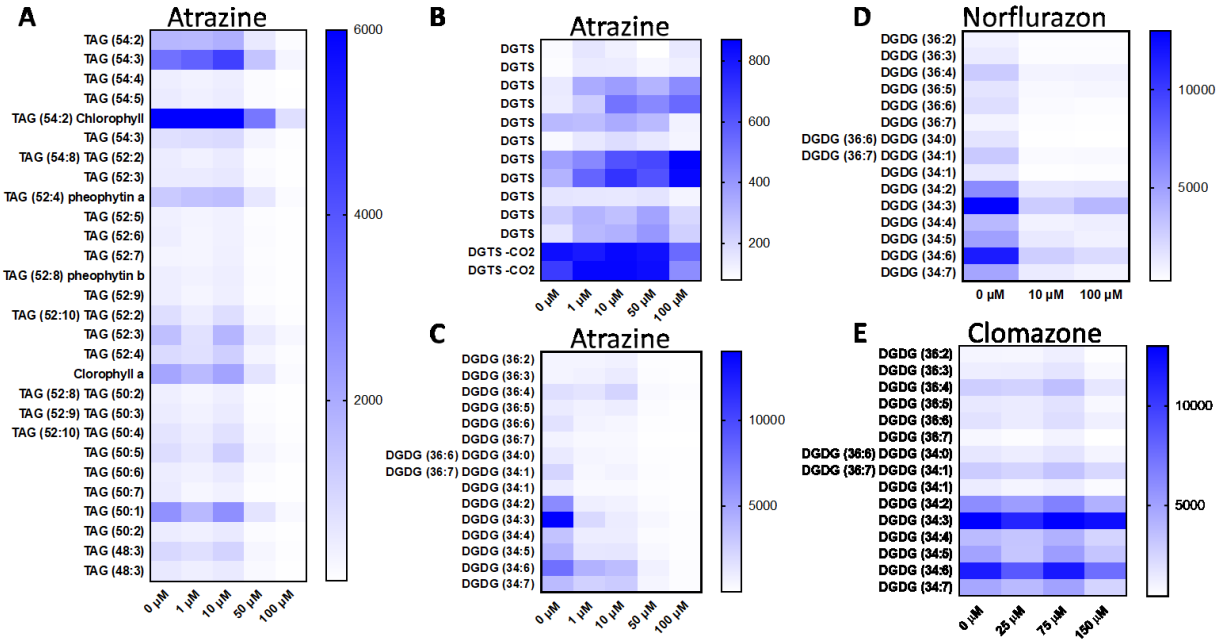

Figure 5. Heat maps of lipid abundance based on lipid species and concentration of herbicide exposure. Exposure doses are indicated along the x-axis for corresponding lipid species along the y-axis of the heat maps. Colored legends along the right side of the heatmaps show the averaged peak intensity of lipid from low (white) to high intensity (dark blue). Atrazine's effect on TAG lipid species (A), on DGTS lipid species (B), and on DGDG lipid species (C). Norflurazon's effect on DGDG lipid species (D) and clomazone's effect on DGDG lipid species (E).

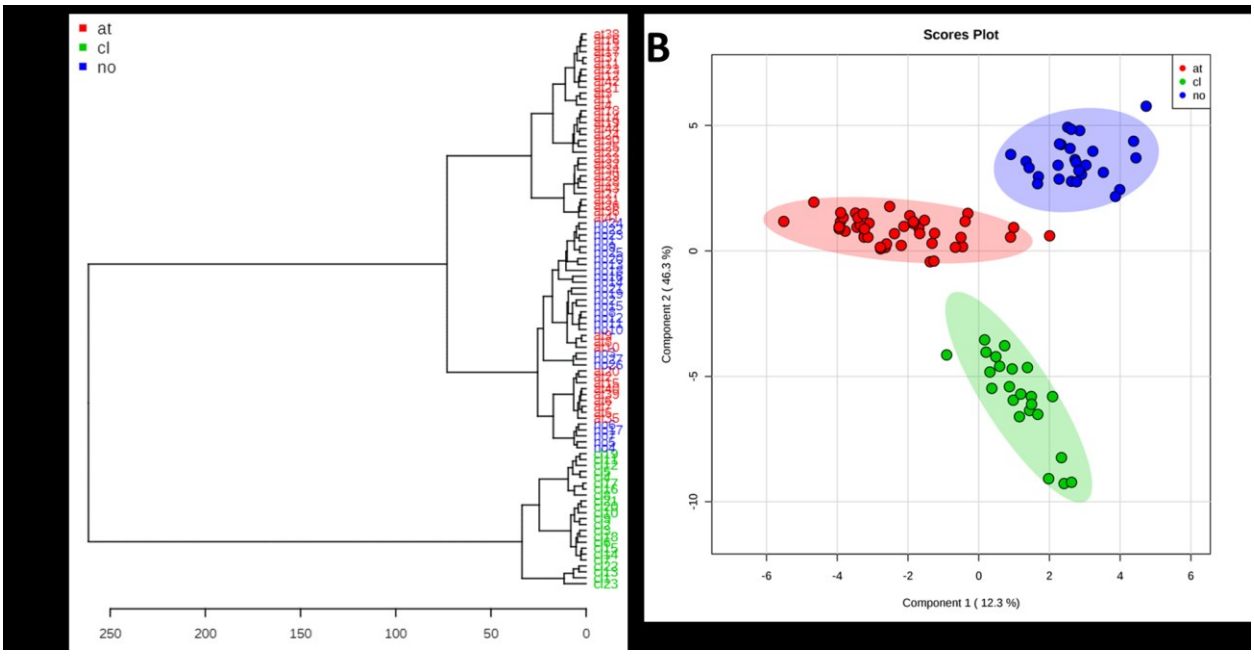

Figure 6. Dendrogram representation of hierarchical similarities between single cells, and PLS-DA maximizes the covariance between X (data) and Y (group) and is often used in the analysis of large biological datasets. The variance displayed in the plot above is the explained variance for X. A pronounced separation is revealed between the three groups of data. Ellipses indicate 95% confidence fitting.

Reference:

1. Walker;, C. H.; Sibly;, R. M.; Hopkin;, S. P.; Peakall, D. B., *Principles of ecotoxicology*. 4 ed.; CRC Press: 2012.
2. Walker, C.; Sibly, R.; Hopkin, S.; Peakall, D., *Principles of Ecotoxicology*. CRC Press: 2012.
3. Ackerman, F., The economics of atrazine. *Int J Occup Env Heal* **2007,** *13* (4), 437-445.
4. Choudri, B. S.; Charabi, Y.; Ahmed, M., Pesticides and Herbicides. *Water Environ Res* **2018,** *90* (10), 1663-1678.
5. Zhang, X. W.; Xia, P.; Wang, P. P.; Yang, J. H.; Baird, D. J., Omics Advances in Ecotoxicology. *Environ Sci Technol* **2018,** *52* (7), 3842-3851.
6. Teo, C. C.; Chong, W. P. K.; Tan, E.; Basri, N. B.; Low, Z. J.; Ho, Y. S., Advances in sample preparation and analytical techniques for lipidomics study of clinical samples. *Trac-Trend Anal Chem* **2015,** *66*, 1-18.
7. Rustam, Y. H.; Reid, G. E., Analytical Challenges and Recent Advances in Mass Spectrometry Based Lipidomics. *Anal Chem* **2018,** *90* (1), 374-397.
8. Jurowski, K.; Kochan, K.; Walczak, J.; Baranska, M.; Piekoszewski, W.; Buszewski, B., Comprehensive review of trends and analytical strategies applied for biological samples preparation and storage in modern medical lipidomics: State of the art. *Trac-Trend Anal Chem* **2017,** *86*, 276-289.
9. Lewis, M.; Thursby, G., Aquatic plants: Test species sensitivity and minimum data requirement evaluations for chemical risk assessments and aquatic life criteria development for the USA. *Environ Pollut* **2018,** *238*, 270-280.
10. Scanlan, L. D.; Loguinov, A. V.; Teng, Q.; Antczak, P.; Dailey, K. P.; Nowinski, D. T.; Kornbluh, J.; Lin, X. X.; Lachenauer, E.; Arai, A.; Douglas, N. K.; Falciani, F.; Stapleton, H. M.; Vulpe, C. D., Gene transcription, metabolite and lipid profiling in eco-indicator daphnia magna indicate diverse mechanisms of toxicity by legacy and emerging flame-retardants. *Environ Sci Technol* **2015,** *49* (12), 7400-10.
11. Blanksby, S. J.; Mitchell, T. W., Advances in Mass Spectrometry for Lipidomics. *Annu Rev Anal Chem* **2010,** *3*, 433-465.
12. Holcapek, M.; Liebisch, G.; Ekroos, K., Lipidomic Analysis. *Anal Chem* **2018,** *90* (7), 4249-4257.
13. Checa, A.; Bedia, C.; Jaumot, J., Lipidomic data analysis: tutorial, practical guidelines and applications. *Anal Chim Acta* **2015,** *885*, 1-16.
14. Yang, K.; Han, X., Lipidomics: Techniques, Applications, and Outcomes Related to Biomedical Sciences. *Trends Biochem Sci* **2016,** *41* (11), 954-969.
15. Kind, T.; Liu, K. H.; Lee, D. Y.; DeFelice, B.; Meissen, J. K.; Fiehn, O., LipidBlast in silico tandem mass spectrometry database for lipid identification. *Nat Methods* **2013,** *10* (8), 755-8.
16. Sud, M.; Fahy, E.; Cotter, D.; Brown, A.; Dennis, E. A.; Glass, C. K.; Merrill, A. H.; Murphy, R. C.; Raetz, C. R. H.; Russell, D. W.; Subramaniam, S., LMSD: LIPID MAPS structure database. *Nucleic Acids Res* **2007,** *35*, D527-D532.
17. Vieler, A.; Wilhelm, C.; Goss, R.; Suss, R.; Schiller, J., The lipid composition of the unicellular green alga Chlamydomonas reinhardtii and the diatom Cyclotella meneghiniana investigated by MALDI-TOF MS and TLC. *Chem Phys Lipids* **2007,** *150* (2), 143-55.

18. Falck, D.; Haberger, M.; Plomp, R.; Hook, M.; Bulau, P.; Wuhrer, M.; Reusch, D., Affinity purification of erythropoietin from cell culture supernatant combined with MALDI-TOF-MS analysis of erythropoietin N-glycosylation. *Sci Rep* **2017,** *7* (1), 5324.
19. Manikandan, M.; Wu, H. F., Bio-mimicked gold nanoparticles with complex fetal bovine serum as sensors for single cell MALDI MS of cancer cell and cancer stem cell. *Sensor Actuat B-Chem* **2016,** *231*, 154-165.
20. Tracey, T. J.; Steyn, F. J.; Wolvetang, E. J.; Ngo, S. T., Neuronal Lipid Metabolism: Multiple Pathways Driving Functional Outcomes in Health and Disease. *Front Mol Neurosci* **2018,** *11*, 10.
21. Zenobi, R., Single-Cell Metabolomics: Analytical and Biological Perspectives. *Science* **2013,** *342* (6163), 1201-+.
22. Ibanez, A. J.; Fagerer, S. R.; Schmidt, A. M.; Urban, P. L.; Jefimovs, K.; Geiger, P.; Dechant, R.; Heinemann, M.; Zenobi, R., Mass spectrometry-based metabolomics of single yeast cells. *P Natl Acad Sci USA* **2013,** *110* (22), 8790-8794.
23. Rahi, P.; Prakash, O.; Shouche, Y. S., Matrix-Assisted Laser Desorption/Ionization Time-of-Flight Mass-Spectrometry (MALDI-TOF MS) Based Microbial Identifications: Challenges and Scopes for Microbial Ecologists. *Front Microbiol* **2016,** *7*, 1359.
24. Lu, J. J.; Tsai, F. J.; Ho, C. M.; Liu, Y. C.; Chen, C. J., Peptide Biomarker Discovery for Identification of Methicillin-Resistant and Vancomycin-Intermediate Staphylococcus aureus Strains by MALDI-TOF. *Anal Chem* **2012,** *84* (13), 5685-5692.
25. Krismer, J.; Sobek, J.; Steinhoff, R. F.; Fagerer, S. R.; Pabst, M.; Zenobi, R., Screening of Chlamydomonas reinhardtii Populations with Single-Cell Resolution by Using a High-Throughput Microscale Sample Preparation for Matrix-Assisted Laser Desorption Ionization Mass Spectrometry. *Appl Environ Microb* **2015,** *81* (16), 5546-5551.
26. Krismer, J.; Steinhoff, R. F.; Zenobi, R., Single-cell MALDI Tandem Mass Spectrometry: Unambiguous Assignment of Small Biomolecules from Single Chlamydomonas reinhardtii Cells. *Chimia* **2016,** *70* (4), 236-239.
27. Krismer, J.; Tamminen, M.; Fontana, S.; Zenobi, R.; Narwani, A., Single-cell mass spectrometry reveals the importance of genetic diversity and plasticity for phenotypic variation in nitrogen-limited Chlamydomonas. *Isme J* **2017,** *11* (4), 988-998.
28. Shanta, P. V.; Li, B.; Stuart, D. D.; Cheng, Q., Plasmonic Gold Templates Enhancing Single Cell Lipidomic Analysis of Microorganisms. *Anal Chem* **2020,** *92* (9), 6213-6217.
29. Sasso, S.; Stibor, H.; Mittag, M.; Grossman, A. R., From molecular manipulation of domesticated Chlamydomonas reinhardtii to survival in nature. *eLife* **2018,** *7*, e39233.
30. Abbas, A.; Linman, M. J.; Cheng, Q., Patterned resonance plasmonic microarrays for high-performance SPR imaging. *Anal Chem* **2011,** *83* (8), 3147-52.
31. Kaya, T.; Kaneko, T.; Kojima, S.; Nakamura, Y.; Ide, Y.; Ishida, K.; Suda, Y.; Yamashita, K., High-sensitivity immunoassay with surface plasmon field-enhanced fluorescence spectroscopy using a plastic sensor chip: application to quantitative analysis of total prostate-specific antigen and GalNAcbeta1-4GlcNAc-linked prostate-specific antigen for prostate cancer diagnosis. *Anal Chem* **2015,** *87* (3), 1797-803.
32. Jing Liu; Rolf Lauterbach; Harald Paulsen; Knoll, W., Immobilization of Light-Harvesting Chlorophyll a/b Complex
(LHCIIb) Studied by Surface Plasmon Field-Enhanced Fluorescence Spectroscopy. *Langmuir* **2008,** *24*, 9661-9667.

33. Liebermann, T. K., W.,, Surface-plasmon field-enhanced fluorescence spectroscopy. *Colloid Surface A* **2000,** *171* (1-3), 115-130.
34. Jicheng Duan; Matthew J. Linman; Cheng, Q., Ultrathin Calcinated Films on a Gold Surface for
Highly Effective Laser Desorption/Ionization of
Biomolecules. *Anal Chem* **2010,** *82*, 5088–5094.
35. Pilolli, R. P., F.; Cioffi, N.,, Gold nanomaterials as a new tool for bioanalytical applications of laser desorption ionization mass spectrometry. *Anal Bioanal Chem* **2012,** *402* (2), 601-623.
36. Chong, J.; Soufan, O.; Li, C.; Caraus, I.; Li, S. Z.; Bourque, G.; Wishart, D. S.; Xia, J. G., MetaboAnalyst 4.0: towards more transparent and integrative metabolomics analysis. *Nucleic Acids Res* **2018,** *46* (W1), W486-W494.
37. Blann, K. L.; Anderson, J. L.; Sands, G. R.; Vondracek, B., Effects of Agricultural Drainage on Aquatic Ecosystems: A Review. *Crit Rev Env Sci Tec* **2009,** *39* (11), 909-1001.
38. Gilliom, R. J.; Barbash, J. E.; Crawford, C. G.; Hamilton, P. A.; Martin, J. D.; Nakagaki, N.; Nowell, L. H.; Scott, J. C.; Stackelberg, P. E.; Thelin, G. P. *Pesticides in the Nation's Streams and Ground Water, 1992-2001*; 1411309553; US Geological Survey: 2006.
39. Gilliom, R. J., Pesticides in U.S. streams and groundwater. *Environ Sci Technol* **2007,** *41* (10), 3407-3413.
40. Choquette, A. F., Pesticides and Nitrate in Groundwater Underlying Citrus Croplands, Lake Wales Ridge, Central Florida, 1999–2005. U.S. Geological Survey Open-File Report 2013–1271, 2014; Vol. 28 p.
41. Fischer, B. B.; Rufenacht, K.; Dannenhauer, K.; Wiesendanger, M.; Eggen, R. I., Multiple stressor effects of high light irradiance and photosynthetic herbicides on growth and survival of the green alga Chlamydomonas reinhardtii. *Environ Toxicol Chem* **2010,** *29* (10), 2211-9.
42. Kabra, A. N.; Ji, M. K.; Choi, J.; Kim, J. R.; Govindwar, S. P.; Jeon, B. H., Toxicity of atrazine and its bioaccumulation and biodegradation in a green microalga, Chlamydomonas mexicana. *Environ Sci Pollut Res Int* **2014,** *21* (21), 12270-8.
43. Yasuor, H.; TenBrook, P. L.; Tjeerdema, R. S.; Fischer, A. J., Responses to clomazone and 5-ketoclomazone by Echinochloa phyllopogon resistant to multiple herbicides in Californian rice fields. *Pest Manag Sci* **2008,** *64* (10), 1031-9.
44. Scupakova, K.; Balluff, B.; Tressler, C.; Adelaja, T.; Heeren, R. M. A.; Glunde, K.; Ertaylan, G., Cellular resolution in clinical MALDI mass spectrometry imaging: the latest advancements and current challenges. *Clin Chem Lab Med* **2020,** *58* (6), 914-929.
45. Do, T. D.; Comi, T. J.; Dunham, S. J. B.; Rubakhin, S. S.; Sweedler, J. V., Single Cell Profiling Using Ionic Liquid Matrix-Enhanced Secondary Ion Mass Spectrometry for Neuronal Cell Type Differentiation. *Anal Chem* **2017,** *89* (5), 3078-3086.
46. Taylor, M. J.; Lukowski, J. K.; Anderton, C. R., Spatially Resolved Mass Spectrometry at the Single Cell: Recent Innovations in Proteomics and Metabolomics. *J Am Soc Mass Spectrom* **2021,** *32* (4), 872-894.
47. Xie, T. T.; Liu, Q.; Cai, W. P.; Chen, Z.; Li, Y. Q., Surface plasmon-coupled directional emission based on a conformational-switching signaling aptamer. *Chem Commun* **2009,** (22), 3190-3192.

48. Cao, S. H.; Cai, W. P.; Liu, Q.; Xie, K. X.; Weng, Y. H.; Huo, S. X.; Tian, Z. Q.; Li, Y. Q., Label-Free Aptasensor Based on Ultrathin-Linker-Mediated Hot-Spot Assembly To Induce Strong Directional Fluorescence. *J Am Chem Soc* **2014,** *136* (19), 6802-6805.
49. Liebermann, T.; Knoll, W., Surface-plasmon field-enhanced fluorescence spectroscopy. *Colloids and Surfaces a-Physicochemical and Engineering Aspects* **2000,** *171* (1-3), 115-130.
50. Jeong, Y.; Kook, Y. M.; Lee, K.; Koh, W. G., Metal enhanced fluorescence (MEF) for biosensors: General approaches and a review of recent developments. *Biosens Bioelectron* **2018,** *111*, 102-116.
51. Almeida, A. C.; Gomes, T.; Langford, K.; Thomas, K. V.; Tollefsen, K. E., Oxidative stress in the algae Chlamydomonas reinhardtii exposed to biocides. *Aquat Toxicol* **2017,** *189*, 50-59.
52. Franz, A. K.; Danielewicz, M. A.; Wong, D. M.; Anderson, L. A.; Boothe, J. R., Phenotypic Screening with Oleaginous Microalgae Reveals Modulators of Lipid Productivity. *Acs Chem Biol* **2013,** *8* (5), 1053-1062.
53. Vieler, A.; Wilhelm, C.; Goss, R.; Sub, R.; Schiller, J., The lipid composition of the unicellular green alga Chlamydomonas reinhardtii and the diatom Cyclotella meneghiniana investigated by MALDI-TOF MS and TLC. *Chem Phys Lipids* **2007,** *150* (2), 143-155.
54. Yang, D. W.; Song, D. H.; Kind, T.; Ma, Y.; Hoefkens, J.; Fiehn, O., Lipidomic Analysis of Chlamydomonas reinhardtii under Nitrogen and Sulfur Deprivation. *Plos One* **2015,** *10* (9), e0137948.
55. Legeret, B.; Schulz-Raffelt, M.; Nguyen, H. M.; Auroy, P.; Beisson, F.; Peltier, G.; Blanc, G.; Li-Beisson, Y., Lipidomic and transcriptomic analyses of Chlamydomonas reinhardtii under heat stress unveil a direct route for the conversion of membrane lipids into storage lipids. *Plant Cell Environ* **2016,** *39* (4), 834-847.
56. Yao, L. X.; Gerde, J. A.; Lee, S. L.; Wang, T.; Harrata, K. A., Microalgae Lipid Characterization. *J Agr Food Chem* **2015,** *63* (6), 1773-1787.
57. Danielewicz, M. A.; Anderson, L. A.; Franz, A. K., Triacylglycerol profiling of marine microalgae by mass spectrometry. *J Lipid Res* **2011,** *52* (11), 2101-2108.
58. Liu, B.; Vieler, A.; Li, C.; Daniel Jones, A.; Benning, C., Triacylglycerol profiling of microalgae Chlamydomonas reinhardtii and Nannochloropsis oceanica. *Bioresour Technol* **2013,** *146*, 310-316.
59. Stringano, E.; Cramer, R.; Hayes, W.; Smith, C.; Gibson, T.; Mueller-Harvey, I., Deciphering the complexity of sainfoin (Onobrychis viciifolia) proanthocyanidins by MALDI-TOF mass spectrometry with a judicious choice of isotope patterns and matrixes. *Anal Chem* **2011,** *83* (11), 4147-53.
60. Strohalm, M.; Kavan, D.; Novak, P.; Volny, M.; Havlicek, V., mMass 3: A Cross-Platform Software Environment for Precise Analysis of Mass Spectrometric Data. *Anal Chem* **2010,** *82* (11), 4648-4651.
61. Nussberger, S.; Dorr, K.; Wang, D. N.; Kuhlbrandt, W., Lipid-protein interactions in crystals of plant light-harvesting complex. *J Mol Biol* **1993,** *234* (2), 347-56.
62. Allakhverdiev, S. I.; Awai, K.; Benning, C.; Block, M. A.; Brown, A. P.; Browse, J.; Cahoon, E. B.; Charuvi, D.; Chen, M.; Chuartzman, S. G.; Dörmann, P.; Dubots, E.; Frentzen, M.; Gavilanes-Ruíz, M.; Giavalisco, P.; Goss, R.; Guskov, A.; Hölzl, G.; Jouhet, J.; Kern, J.; Kinney, A. J.; Kirchhoff, H.; Krauss, N.; Lechno-Yossef, S.; Los, D. A.; Maréchal, E.; Meyer, K.; Miller, R.; Mizusawa, N.; Moellering, E. R.; Mullineaux, C. W.; Murata, N.; Nakamura, Y.; Nevo, R.; Ohta, H.; Plasencia, J.; Rafferty, J. B.; Reich, Z.; Sadre, R.; Sato,

N.; Saucedo-García, M.; Seiwert, B.; Shimojima, M.; Shimoni, E.; Slabas, A. R.; Tsabari, O.; Wada, H.; Wilhelm, C.; Willmitzer, L.; Wolk, C. P.; Zinchenko, V. V.; Zouni, A., *Lipids in Photosynthesis Essential and Regulatory Functions*. Springer: 2009; Vol. 30.
63. Li, Y.; Horsman, M.; Wu, N.; Lan, C. Q.; Dubois-Calero, N., Biofuels from microalgae. *Biotechnol Prog* **2008,** *24* (4), 815-20.
64. Anderson, L. A., *Chemical Stimulation of Lipid Production in Microalgae and Analysis by NMR Spectroscopy for Biofuel Applications*. University of California, Davis: 2015.
65. Breitenbach, J.; Zhu, C. F.; Sandmann, G., Bleaching herbicide norflurazon inhibits phytoene desaturase by competition with the cofactors. *J Agr Food Chem* **2001,** *49* (11), 5270-5272.
66. Ferhatoglu, Y.; Barrett, M., Studies of clomazone mode of action. *Pestic Biochem Phys* **2006,** *85* (1), 7-14.

TOC Graphic

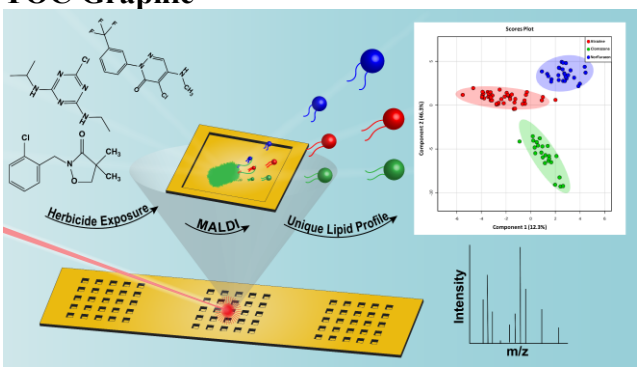
Herbicide Exposure
MALDI
Unique Lipid Profile
Intensity
m/z